Case Report

Paraneoplastic opsoclonus-myoclonus syndrome secondary to melanoma metastasis form occult primary cancer

Jaime D. Mondragón[a, b]   Omar Jiménez-Zarazúa[c, d]
Lourdes N. Vélez-Ramírez[e]   María Andrea Martínez-Rivera[c]
Samnir Enríquez-Maciel[f]   Jesús González-Guzmán[f]
Martha Mercedes Alvarez-Delgado[d]   Pedro Luis González-Carrillo[g]

[a]Department of Neurology, University of Groningen, University Medical Center Groningen, Groningen, The Netherlands; [b]University of Groningen, University Medical Center Groningen, Alzheimer Research Center Groningen, Groningen, The Netherlands; [c]Department of Internal Medicine, Hospital General León, León de los Aldama, Mexico; [d]Department of Medicine and Nutrition, Universidad de Guanajuato, Guanajuato, Mexico; [e]Department of Radiology, Hospital General León, León de los Aldama, Mexico; [f]Department of Pathology, Hospital General León, León de los Aldama, Mexico; [g]Department of Critical Care, Hospital General León, León de los Aldama, Mexico

Abstract
Introduction: Opsoclonus-myoclonus syndrome (OMS) is an inflammatory neurological disorder, often requiring a prompt medical evaluation. Among the diverse etiologies associated with OMS are autoimmune, infectious, paraneoplastic, and systemic diseases, and drug intoxication. ***Clinical Summary:*** The case of a 36-year-old female with a disabling holocranial headache, sudden loss of consciousness, aggressive behavior, vertigo, and a personal history of

Jaime D. Mondragón
University Medical Center Groningen
Department of Neurology, PO Box 30001
NL–9700 RB Groningen (The Netherlands)
E-Mail j.d.mondragon.uribe@umcg.nl

KARGER

somatoform disorder and major depression is presented here. After hospital admission, the patient developed sudden stereotyped movements in all four extremities and oculogyric crises compatible with OMS. Cerebrospinal fluid analysis, viral and autoimmune assays, as well as blood, urine, and bronchial secretion cultures, drug metabolite urinalysis, and tumor markers were all negative. Furthermore, brain computed tomography (CT) and brain magnetic resonance imaging, along with thoraco-abdominopelvic CT and electroencephalography, were also all negative. The patient suffered type one respiratory insufficiency after 72 h of hospitalization, requiring an endotracheal tube. After 13 days the patient suffered cardiac arrest. Necropsy was performed reporting lymph nodes with a poorly differentiated malignant neoplastic lesion, HMB-45, melan-A, vimentin, and S-100 positive, compatible with melanoma metastasis from an occult primary cancer. ***Discussion:*** While the incidence of melanoma of unknown primary is between 2.6 and 3.2%, with a median overall survival ranging between 24 and 127 months, when melanoma patients develop OMS their survival is markedly decreased. Although only 5 cases of paraneoplastic OMS secondary to melanoma have been reported in the literature, all had a poor prognosis, dying within 8 months of OMS onset.

© 2019 The Author(s)
Published by S. Karger AG, Basel

Introduction

Opsoclonus-myoclonus syndrome (OMS) is an inflammatory neurological disorder, often requiring an expedient medical evaluation. OMS is also known as opsoclonus-myoclonus-ataxia or myoclonic encephalopathy and as Kinsbourne syndrome when it affects infants and young children [1]. OMS is a rare disease characterized by multidirectional eye movements (i.e., saccades) that are involuntary, arrhythmic, and chaotic [2]. These saccades have different directional components (i.e., horizontal, vertical, and torsional) and are associated with myoclonic limb and trunk sudden movements, cerebellar ataxia, tremor, and encephalopathy [2]. Definitive diagnosis for myoclonus is expensive and time-consuming; furthermore, only a minority of the cases are thoroughly diagnosed [3]. The clinical approach to myoclonus diagnosis involves electrophysiological, imaging, and laboratory tests [3]. Among the etiologies associated with myoclonus are infectious, autoimmune, medications and toxic agents, paraneoplastic, central nervous system lesions, metabolic diseases, and prion disease [3].

We present the clinicopathological case of a patient with sudden stereotyped movements in all four extremities and oculogyric crises compatible with OMS. After infectious and post-infectious etiologies were excluded the patient was screened for autoimmune and drug-related etiologies, without success. The patient was screened for a neoplastic process through imaging and tumor makers, but the results were still negative. After an axillary lymph node biopsy, the diagnosis of melanoma was established. Paraneoplastic OMS secondary to melanoma is a very rare presentation and prompt tumor diagnosis is needed in order to provide adequate care for the patient based on their prognosis and overall survival.

Clinical Presentation

A 36-year-old female arrived at the Emergency Department presenting a sudden loss of consciousness secondary to head trauma after falling from her own height on two episodes. After the second fall, the patient had loss of strength in the lower extremities leading to impaired ambulation. The patient had a sudden-onset disabling holocranial headache, aggressive behavior, and vertigo for the 2 weeks prior to her arrival at the Emergency Department. The patient did not have any symptoms related to an acute infectious process (e.g., fever or malaise). She sought out medical attention at a regional psychiatric hospital from which she was referred to our institution with a somatoform disorder and depressive episode diagnosis. The patient's family history included a father deceased secondary to type 2 diabetes and colon cancer complications; no other relevant aspects of family history were found. The patient denied the use of controlled substances, allergies, past blood transfusions, traveling to regions with endemic diseases within the last 3 months, tattoos, and body piercings. The patient had three pregnancies, three deliveries, and no cesarean surgeries, without any psychological or physiological complications with regard to her past obstetric history. She was diagnosed with major depression 18 months prior to admission to this hospital; however, she had no adherence to medical treatment and two previous suicide attempts within this time period.

Upon initial physical exploration, we found a recumbent patient with freely chosen body position, Glasgow coma score of 11 (i.e., eye-opening 4, verbal response 1, motor response 6), without focal neurologic deficits or meningeal sings, aware of her environment but with mutism, and without making verbal or eye contact. The patient's integumentary system was hydrated and without alterations. She had horizontal nystagmus associated with oculogyric crises, while the rest of the head and neck exploration had no alterations. Fundus examination was not performed due to the excessive saccadic eye movements. The musculoskeletal exploration revealed stereotyped movements in all four extremities, which had an onset of a couple of hours. The patient had normal plantar and other deep tendon reflexes. Cerebellar function and muscle strength were not evaluated due to the patient's lack of cooperation. Upon inspection, auscultation, and percussion the cardio-respiratory system had no abnormal findings. During thoracic palpation, a mass (2 × 2 × 3 cm, petrous consistency, and immobile) in the right axillar line was detected. No abnormalities were found on breast examination. Abdominal examination was without alterations. Upon admission, the patient had the following vital signs: blood pressure of 94/60 mm Hg; heart rate of 77 bpm; respiratory rate of 20 rpm; temperature of 36.5°C; body-weight of 60 kg; height of 158 cm; and BMI of 24.0.

Clinical Evolution

The patient was evaluated by the psychiatry department confirming the somatoform disorder and depressive episode diagnosis, providing management with olanzapine and sertraline. The neurology department evaluated the patient to assess the sudden-onset movement disorder integrating an OMS. Initial diagnosis suspicion was post-viral cerebellar ataxia or neuroinfectious disease. Laboratory results at admission are presented in Table 1. A computed tomography (CT) of the brain was performed to assess intra-axial lesions (e.g., hemorrhage, ischemia, and tumors) with normal findings. The cerebrospinal fluid analysis was normal (Table 1). Management with alprazolam and magnesium valproate was initiated to address the psychomotor agitation and movement disorder. The urinalysis was compatible with

a urinary tract infection (Table 2) which was treated with intravenous ceftriaxone. Blood, bronchial secretion, and urine cultures were performed, with all cultures reporting negative results. To exclude viral infection or drug use the following tests were requested: antibodies for hepatitis B virus, hepatitis C virus, and HIV, as well as urinalysis for benzodiazepines, barbiturates, cannabis, cocaine, methamphetamines, and opiates; all results were reported as negative (Table 2). Procalcitonin serum levels were 1.67 ng/mL. After an infectious etiology was excluded, an electroencephalogram was performed, yielding no epileptogenic or abnormal activity. In search of an autoimmune etiology, the following tests were requested: cytoplasmic antineutrophil cytoplasmatic antibodies, perinuclear antineutrophil cytoplasmatic antibodies, anti-double-stranded deoxyribonucleic acid, anti-cardiolipin IgG, anti-cardiolipin IgM antibody, and anti-N-methyl-D-aspartate receptor, all reported as negative (Table 2).

Screening for a neoplastic process in the brain, magnetic resonance imaging (Fig. 1a, b) was performed, reporting normal results. The following tumor markers were screened and all were reported negative: alpha-fetoprotein, human chorionic gonadotropin, CA125, CA153, CA19.9, and carcinoembryonic antigen (Table 2). An axillary ganglion biopsy was performed reporting a high-grade and poorly differentiated malignancy (Fig. 2a, b). Immunohistochemical staining with cytokeratin AE1/AE3, CD 45, Cyclin D1, CD 117, smooth muscle actin-alpha, and BCL2 were all reported as negative, while staining for HMB-45, melan-A, vimentin, and S-100 were positive. The histopathological diagnosis was compatible with melanoma (Fig. 2c–f). In search of a primary site simple and contrasted thoracic, abdominal, and pelvic CTs were performed (Fig. 1c–f). No primary site or apparent lymphadenopathy were identified. The CT of the thorax showed lung parenchyma with areas of consolidation and images compatible with ground glass opacities and air bronchogram (Fig. 1c, d). To further search for a primary site a positron emission tomography (PET) was scheduled.

Clinical Outcome

Seventy-two hours after admission, the patient developed type one respiratory insufficiency (i.e. vital signs: blood pressure of 90/60 mm Hg; heart rate of 120 bpm, respiratory rate of 27 rpm, temperature of 39°C; blood gas test arterial pH = 7.3, PaO_2 = 50 mm Hg, $PaCO_2$ = 30 mm Hg, HCO_3^- = 18 mEq/L, O_2 content = 75%, base excess = –6 mmol/L; lactate = 0.9 mmol/L), thus requiring invasive artificial airway with an endotracheal tube and admittance to the Intensive Care Unit for further test and treatment. The patient had a torpid evolution characterized by purulent bronchial secretions, 39°C body temperature and increase in leucocyte count (Table 2). The microorganism *Acinetobacter baumannii* was isolated from the bronchial secretion (i.e. >100,000 colony-forming units/mL). Intravenous colistimethate and meropenem were initiated. Due to the septic process, the PET imaging was not performed.

After 13 days of hospitalization, the patient presented extreme bradycardia (40 BPM), progressing to asystole. Advanced life support protocol was initiated and after 20 min without reverting the cardiac arrest the patient was pronounced deceased. Necropsy examination was performed by two independent pathologists reporting hemorrhagic lesions at the corpus callosum level, multiple paratracheal and perihilar lymph nodes (e.g. sizes ranging from 0.8 × 0.5 cm and 1.5 × 1.2 cm) (Fig. 3). The histological sections of the axillary, paratracheal and perihilar lymph nodes showed a poorly differentiated malignant neoplastic lesion constituted by pleomorphic cells, atypical nuclei with open chromatin, nuclear pseudo-inclusions, and mitosis (Fig. 2a, b, 3c, d). Immunohistochemical staining was performed and antibodies for HMB-

45, melan-A, vimentin, and S-100 were positive (Fig. 2c–f). Both pathologists reached the same diagnosis and were unable to identify the primary site. The final diagnosis was melanoma metastasis from an occult primary cancer.

Discussion

To the best of the authors' knowledge, this is the first case reported in the literature involving a paraneoplastic OMS secondary to melanoma metastasis from an occult primary cancer and just the fifth case involving melanoma. The first case of paraneoplastic OMS secondary to malignant melanoma was described in 1999 by Berger and Mehari [4] (1999), where the male patient had a previous history of malignant melanoma (left shoulder) which progressed to a recurrent metastatic melanoma with neurological deterioration after 4 months. The second case of OMS secondary to melanoma (vaginal melanoma) reported in the literature describes a female patient that had a sudden onset OMS which progressed to a coma within 2 weeks [5]. The third case reported in the literature was also a vaginal melanoma with abrupt onset of neurological symptoms with rapid neurological deterioration with improvement after 6 weeks but ultimately succumbing to the disease after 6 months [6]. The fourth case involves a male patient with an advanced malignant melanoma (mucosal melanoma in the nasal cavity) who was first diagnosed with a post-infectious OMS but after neurological deterioration died 8 months after the onset of neurological symptoms [7]. All cases including the one reported here have had a poor prognosis, leading to death within 8 months of the movement disorder onset.

This is the first case in the literature of paraneoplastic OMS that was diagnosed through the biopsy of a metastatic site in vivo and confirmed through a necropsy. After imaging, serological, cerebrospinal fluid analysis, and necropsy by two independent pathologists, the primary site was not identified; thus, a final diagnosis of melanoma metastasis from an occult primary cancer was reached. Among the neoplasms of unknown primary origin, differentiated adenocarcinoma corresponds to 60%, poorly differentiated to 30%, undifferentiated to 5%, and squamous cell carcinoma to 5% [8]. From a histopathologic perspective, the pathologic approach to metastases of unknown primary cancer is stepwise and should incorporate the clinical context, morphology, and immunohistochemistry [9]. Primary tumor site prediction can be assisted by the diagnosis of malignancy and broad tumor typing (i.e., into carcinoma, melanoma, lymphoma, or sarcoma) of an occult primary neoplasm [9]. In a study evaluating over 132 thousand patients with melanoma, the incidence of melanoma of unknown primary (MUP) was 3.2%, with a median overall survival ranging between 24 and 127 months, a 5-year survival rate between 28.6 and 75.6%, and a 10-year survival rate between 18.8 and 62.9% for patients having lymph node metastasis [10]. The survival of fewer than 8 months in the 5 OMS cases associated with melanoma is markedly less compared with the overall survival of 24 and 127 months for MUP alone. Another population-based study reported an incidence of 2.6% in a population of over 33 thousand melanoma patients [11]. In this study, the authors report that MUP patients with 2 or more involved lymph nodes had slightly worse survival than patients with tumor-node-metastasis stage III melanoma of a known primary origin [11]. In the clinicopathological case presented above, 6 lymphatic nodes had metastasis, thus contributing to the overall poor prognosis.

Limitations

One of the limitations regarding the diagnostic algorithm in the case presented here was the lack of PET imaging. This imaging modality was not performed on the patient due to the sudden respiratory failure and subsequent septic process. This imaging modality could have assisted in detecting a possible primary site; however, even after undergoing necropsy the patient's primary cancer site was still unknown. Electrophysiological testing (i.e., polymyography, electromyography, and somatosensory evoked potential) to classify the myoclonus were not performed in the patient due to the rapid neurological deterioration and sudden respiratory failure.

Conclusion

Adult-onset OMS is rare. Paraneoplastic and parainfectious causes are the most commonly identified etiologies and should be initially considered in adult-onset OMS [12]. Although complete remission in OMS is commonly achieved with immunotherapy, when OMS is associated with either melanoma of a known primary origin or MUP the survival is markedly reduced [12]. Considering that OMS secondary to melanoma is rare, the available literature and this clinicopathological case report suggest that paraneoplastic OMS associated with melanoma has a poor survival.

## Acknowledgments

Statement of Ethics

Approval from the ethics committee was not required due to the nature of this case report. Abiding by the Declaration of Helsinki, patient anonymity was guaranteed. Upon hospital admission, the patient signed an informed consent permitting the use of her clinical file information for didactic and research purposes.
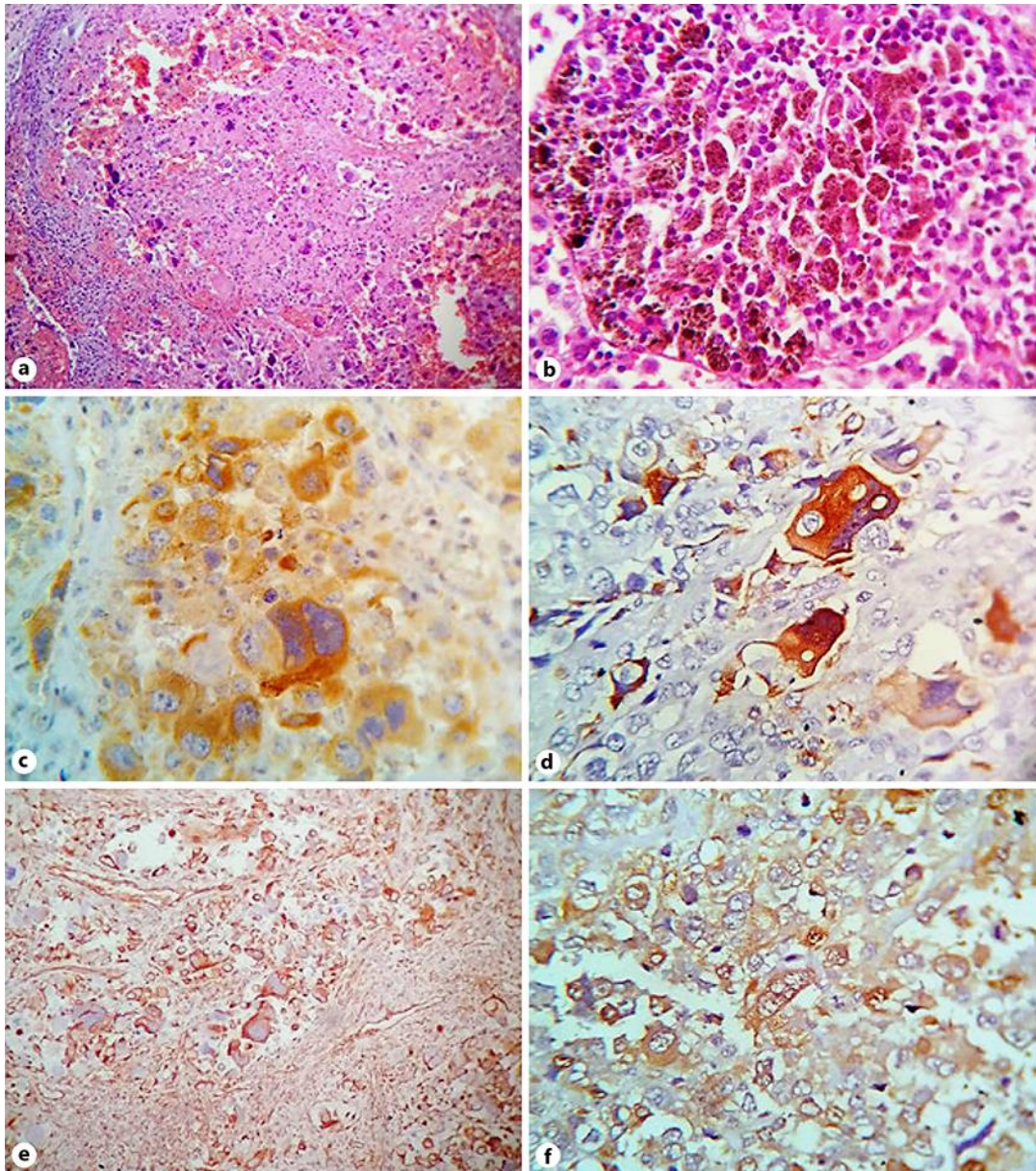
Disclosure Statement

References

1   Pike M. Opsoclonus-myoclonus syndrome. Handb Clin Neurol. 2013;112:1209–11.
2   Wong AM, Musallam S, Tomlinson RD, Shannon P, Sharpe JA. Opsoclonus in three dimensions: oculographic, neuropathologic and modelling correlates. J Neurol Sci. 2001 Aug;189(1-2):71–81.
3   Zutt R, van Egmond ME, Elting JW, van Laar PJ, Brouwer OF, Sival DA, et al. A novel diagnostic approach to patients with myoclonus. Nat Rev Neurol. 2015 Dec;11(12):687–97.
4   Berger JR, Mehari E. Paraneoplastic opsoclonus-myoclonus secondary to malignant melanoma. J Neurooncol. 1999 Jan;41(1):43–5.
5   Jung KY, Youn J, Chung CS. Opsoclonus-myoclonus syndrome in an adult with malignant melanoma. J Neurol. 2006 Jul;253(7):942–3.
6   Hauspy J, Nevin A, Harley I, Mason W, Quirt I, Ghazarian D, et al. Paraneoplastic syndrome in vaginal melanoma: a case report and review of the literature. Int J Gynecol Cancer. 2007 Sep-Oct;17(5):1159–63.
7   Dresco F, Aubin F, Deveza E, Revenco E, Tavernier L, Puzenat E. Paraneoplastic opsoclonus-myoclonus syndrome preceding a mucosal malignant melanoma. Acta Derm Venereol. 2018. https://doi.org/10.2340/00015555-3062.
8   Varadhachary GR, Raber MN. Cancer of unknown primary site. N Engl J Med. 2014 Aug;371(8):757–65.
9   Oien KA. Pathologic evaluation of unknown primary cancer. Semin Oncol. 2009 Feb;36(1):8–37.
10 Kamposioras K, Pentheroudakis G, Pectasides D, Pavlidis N. Malignant melanoma of unknown primary site. To make the long story short. A systematic review of the literature. Crit Rev Oncol Hematol. 2011 May;78(2):112–26.
11 de Waal AC, Aben KK, van Rossum MM, Kiemeney LA. Melanoma of unknown primary origin: a population-based study in the Netherlands. Eur J Cancer. 2013 Feb;49(3):676–83.
12 Klaas JP, Ahlskog JE, Pittock SJ, Matsumoto JY, Aksamit AJ, Bartleson JD, et al. Adult-onset opsoclonus-myoclonus syndrome. Arch Neurol. 2012 Dec;69(12):1598–607.

Mondragón et al.: Paraneoplastic OMS secondary to melanoma metastasis form occult primary cancer
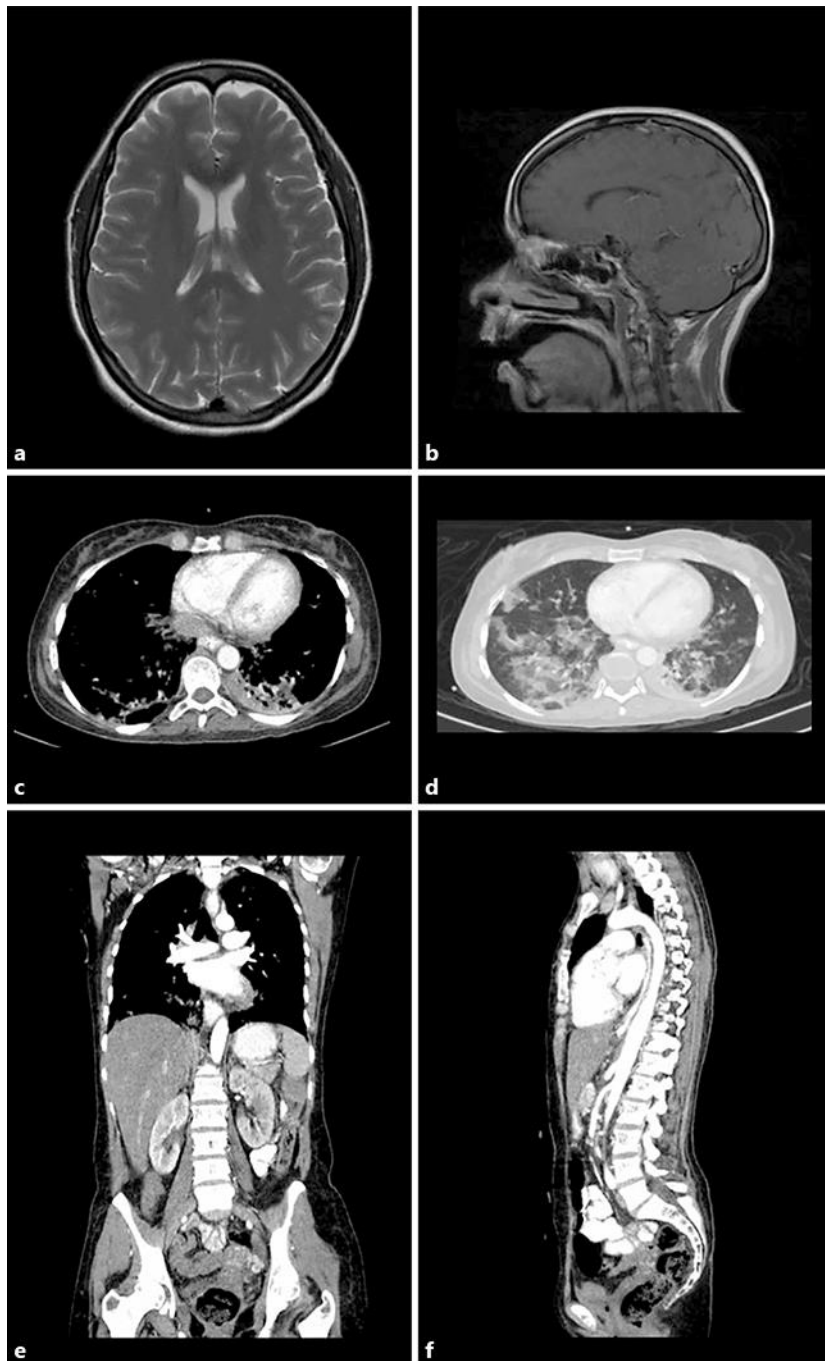
Fig. 1. Brain magnetic resonance imaging (MRI) and thoraco-abdominopelvic computed tomography (CT). **a** Normal axial T2-weighted MRI scan with a thalamic window. **b** Normal sagittal T1-weighted scan with gadolinium with a midbrain window. **c** CT of the thorax without contrast, mediastinal window, a small area of consolidation in both hemithorax with left predominance; this consolidation was accompanied by air bronchogram. **d** CT of the thorax with a lower (basal) plane, where volume asymmetry is observed favoring the right hemithorax, as well as bilateral ground-glass opacities with right predominance. **e** Normal coronal reconstruction of thoraco-abdominopelvic CT with contrast. **f** Normal sagittal thoraco-abdominopelvic CT with contrast.

Mondragón et al.: Paraneoplastic OMS secondary to melanoma metastasis form occult primary cancer

Fig. 2. Histopathology. **a** Axillary ganglion. Hematoxylin and eosin staining. ×50. High-grade and poorly differentiated malignancy. **b** Axillary ganglion. Hematoxylin and eosin staining. ×100. Poorly differentiated malignant neoplastic lesion constituted by pleomorphic cells, atypical nuclei with open chromatin, nuclear pseudo-inclusions, and mitosis. **c–f** Axillary ganglion. ×100. Histopathological diagnosis compatible with melanoma. **c** Melan-A staining positive. **d** HMB-45 staining positive. **e** Vimentin staining positive. **f** S-100 staining positive.

Mondragón et al.: Paraneoplastic OMS secondary to melanoma metastasis form occult primary cancer
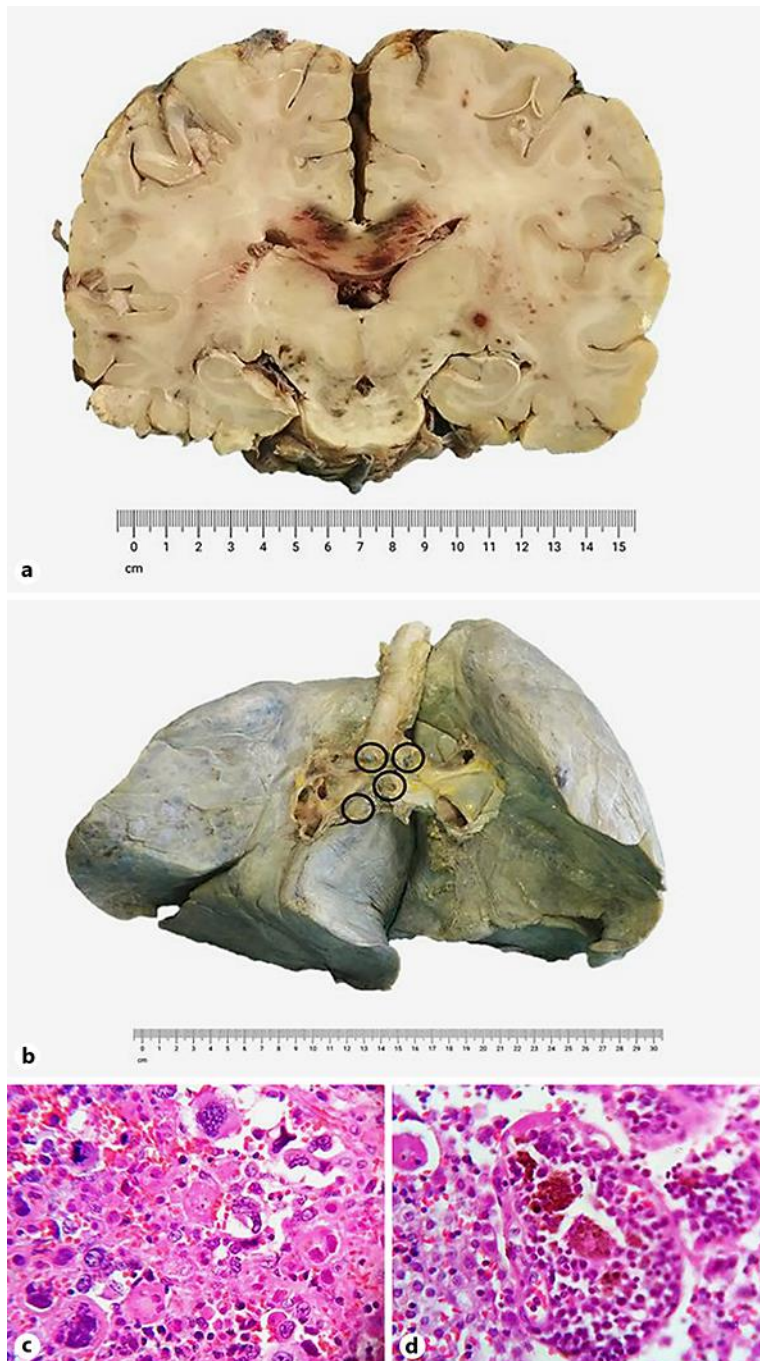
Fig. 3. Necropsy of the brain and lungs. Histopathology of paratracheal and perihilar lymph nodes. **a** Necropsy of the brain. Coronal brain with hemorrhagic lesions at the corpus callosum level. **b** Necropsy of the lungs. Paratracheal and perihilar lymph nodes with sizes ranging from 0.8 × 0.5 cm to 1.5 × 1.2 cm, firm, with solid surface and abundant dark pigment. **c** Histopathology of paratracheal and perihilar lymph nodes. Hematoxylin and eosin staining. ×100. Poorly differentiated malignant neoplastic lesion with nuclear pseudo-inclusions and mitosis. **d** Histopathology of paratracheal and perihilar lymph nodes. Hematoxylin and eosin staining. ×150. Poorly differentiated malignant neoplastic lesion with nuclear pseudo-inclusions and mitosis.

Table 1. Laboratory test results upon admission

Full blood count		Meningitis/encephalitis PCR assay	
Hemoglobin at admission, g/dL	13.6	**Bacteria**	
Hematocrit, %	40.6	*Escherichia coli* K1	Not detected
Erythrocyte count, µL	3,600	*Haemophilus influenzae*	Not detected
Platelet count, µL	1,400	*Listeria monocytogenes*	Not detected
Mean corpuscular volume, fL	91.2	*Neisseria meningitides*	Not detected
Mean corpuscular hemoglobin, g/dL	33.6	*Streptococcus agalactiae*	Not detected
Leukocyte count, µL	8,300	*Streptococcus pneumoniae*	Not detected
Lymphocytes, %	18.1	*Mycobacterium tuberculosis*	Not detected
Neutrophils, %	75.5	**Viruses**	
Monocytes, %	5.9	Cytomegalovirus	Not detected
Eosinophils, %	0.2	Enterovirus	Not detected
Basophils, %	0.3	Herpes simplex virus 1	Not detected
Blood chemistry		Herpes simplex virus 2	Not detected
Glucose, mg/dL	88	Human herpesvirus 6	Not detected
Albumin, g/dL	2.42	Human parechovirus	Not detected
Urea nitrogen, mg/dL	0.47	Varicella zozter virus	Not detected
Blood urea nitrogen, mg/dL	12.6	**Yeast**	
Uric acid, mg/dL	7	*Cryptococcus neoformans/gattii*	Not detected
Cholesterol, mg/dL	130	**Cerebrospinal fluid**	
Triglycerides, mg/dL	140	Aspect	Rock water
Liver function enzymes		Leucocytes	0
Aspartate transaminase, U/L	33	Gram staining	No bacteria
Alanine transaminase, U/L	35	Culture	No development
Lactate dehydrogenase, U/L	160		
Albumin, mg/dL	3.3		
Alkaline phosphatase, U/L	100		
Gamma-glutamyl transpeptidase, U/L	10		
Blood coagulation			
Prothrombine time, s	18		
Partial thromboplastin time, s	40		
International normalized ratio	1.36		
Electrolytes			
Sodium, mEq/dL	139		
Potassium, mE/dL	4.7		
Chlorine, mEq/dL	112		
Calcium, mg/dL	9.7		
Phosphorus, mg/dL	4		
Magnesium, mEq/dL	1.29		

Mondragón et al.: Paraneoplastic OMS secondary to melanoma metastasis form occult primary cancer

Table 2. Follow-up laboratory test results

Full blood count at 13th day of hospitalization	
Platelet count, µL	170,000
Leukocyte count, µL	17,400
Neutrophils, %	97
Lymphocytes, %	2.6
Monocytes, %	0.4
Eosinophils, %	0
Basophils, %	0
Procalcinotine, ng/mL	8
Antibodies	
Cytoplasmic antineutrophil cytoplasmatic antibodies	0.1
Perinuclear antineutrophil cytoplasmatic antibodies	0.2
Anti-double-stranded deoxyribonucleic acid, UI/mL	0.9
Anti-cardiolipin IgG, UI/mL	1.0
Anti-cardiolipin IgM antibody, UI/mL	3.0
Anti-N-methyl-D-aspartate receptor	Negative
Viral panel	
Hepatitis B virus	Negative
Hepatitis C virus	Negative
Human immunodeficiency virus	Negative
Tumor markers	
Alpha-fetoprotein, IU/mL	1,590
Human chorionic gonadotropin, mU/mL	0.31
CA125, UI/mL	34
CA153, UI/mL	5.4
CA19.9, UI/mL	7.4
Carcinoembryonic antigen, ng/mL	1,410
Urinalysis	
Appearance	Cloudy
pH	6.0
Specific gravity	1.032
Proteins, mg/dL	30
Ketones, glucose, and nitrite	Negative
Leukocytes (per high power field)	210
Erythrocytes (per high power field)	400
Bacteria	Abundant